RESEARCH ARTICLE

Dynamic clustering of dynamin-amphiphysin rings regulates membrane constriction and fission coupled with GTP hydrolysis

Tetsuya Takeda[1*], Toshiya Kozai[2], Huiran Yang[1], Daiki Ishikuro[2], Kaho Seyama[1], Yusuke Kumagai[2], Tadashi Abe[1], Hiroshi Yamada[1], Takayuki Uchihashi[4], Toshio Ando[3*], Kohji Takei[1*]

[1]Graduate School of Medicine, Dentistry and Pharmaceutical Sciences, Okayama University, Okayama, Japan; [2]Department of Physics, College of Science and Engineering, Kanazawa University, Kanazawa, Japan; [3]Bio-AFM Frontier Research Center, Institute of Science and Engineering, Kanazawa University, Kanazawa, Japan; [4]Department of Physics, School of Science, Nagoya University

*For correspondence: ttakeda@okayama-u.ac.jp (T.T.), tando@staff.kanazawa-u.ac.jp (T.A.) and kohji@md.okayama-u.ac.jp (K.T.).

ABSTRACT

Dynamin is a mechanochemical GTPase essential for membrane fission during clathrin mediated endocytosis. Dynamin forms washer ring-shaped/helical complexes at the neck of clathrin-coated pits and their structural changes coupled with GTP hydrolysis drive membrane fission. Dynamin and its binding protein amphiphysin cooperatively regulates membrane remodeling during fission, but its precise mechanism remains elusive. In this study, we analyze structural changes of dynamin-amphiphysin complexes during membrane fission using electron microscopy (EM) and high-speed atomic force microscopy (HS-AFM). Interestingly, HS-AFM analyses show that the dynamin-amphiphysin rings are rearranged to form clusters upon GTP hydrolysis and membrane constriction occurs at protein-uncoated regions flanking the clusters. We also show a novel function of amphiphysin in size control of the clusters to enhance biogenesis of endocytic vesicles. Our new approaches using combination of EM and HS-AFM clearly demonstrates dynamics of dynamin-amphiphysin complexes during membrane fission suggesting a novel “clusterase” model of dynamin-mediated membrane fission.

INTRODUCTION

Clathrin mediated endocytosis (CME) is the best characterized endocytic pathway by which cells incorporate extracellular molecules into cells with the aid of clathrin coat (Kirchhausen, Owen, & Harrison, 2014; McMahon & Boucrot, 2011). CME is required for various essential processes including neuronal transmission, signal transduction and other cell membrane activities such as cell adhesion and migration. For precise progression of membrane invagination and fission during CME, various proteins need to be assembled in a temporally and spatially coordinated manner at the site of endocytosis.

One of those endocytic proteins, dynamin, is a GTPase essential for membrane fission in CME (Antonny et al., 2016; Ferguson & De Camilli, 2012; Schmid & Frolov, 2011). There are three dynamin isoforms in mammals: dynamin 1 and dynamin 3, two tissue specific isoforms which are highly expressed in neurons, and dynamin 2, a ubiquitously expressed isoform (Cao, Garcia, & McNiven, 1998; T. Cook, Mesa, & Urrutia, 1996; T. A. Cook, Urrutia, & McNiven, 1994). Structural studies from several groups demonstrated that dynamin consists of five structurally distinct domains: a GTPase domain, a bundle signaling element (BSE), a stalk, a pleckstrin homology (PH) domain and proline-rich domain (PRD) from N-terminus to C-terminus (Faelber et al., 2011; Ford, Jenni, & Nunnari, 2011; Reubold et al., 2015). The GTPase domain is responsible for hydrolysis of GTP (guanosine triphosphate) and PH domain is required for membrane association by binding to negatively charged phospholipids such as PI (4,5) P_2 (phosphatidylinositol 4,5-bisphosphate). The stalk structure serves as a binding interface for dimerization and oligomerization of dynamin, and BSE, which is located between the stalk and GTPase domain, functions as a flexible hinge required for structural changes of dynamin upon GTP hydrolysis. Dynamin forms washer ring-like or helical oligomers which were first observed in presynaptic terminals of *shibire* mutant flies at restrictive temperature (Koenig & Ikeda, 1989). Dynamin also assembles into helices at the neck of endocytic pits in the isolated presynaptic nerve terminals treated with slowly-hydrolyzable GTP analogue GTPγS (guanosine 5'-O-[gamma-thio]triphosphate) (Takei, McPherson, Schmid, & De Camilli, 1995). Similar dynamin rings/helix were reconstituted *in vitro* either with liposomes (Sweitzer & Hinshaw, 1998; Takei et al., 1998) or without liposomes in a low salt condition (Hinshaw & Schmid, 1995).

There is a consensus view about the dynamin-mediated membrane constriction and fission which is well supported by previous studies from different groups: membrane constriction is required, but not sufficient, for fission (Antonny et al., 2016; Faelber et al., 2012; Schmid & Frolov, 2011). However, it is still controversial how constriction is achieved, and what GTP

energy is used for. For example, membrane constriction could be achieved by assembly into the highly-constricted state when dynamin is bound to GTP (Chen, Zhang, Egelman, & Hinshaw, 2004; Mattila et al., 2015; Mears, Ray, & Hinshaw, 2007; Zhang & Hinshaw, 2001). Alternatively, membrane constriction could be achieved by hydrolysis of GTP that induces a conformational change leading to constriction (Cocucci, Gaudin, & Kirchhausen, 2014; Marks et al., 2001; Roux, Uyhazi, Frost, & De Camilli, 2006). However, precise mechanisms involved in dynamin-mediated membrane constriction and fission remain unclear.

Amphiphysin is a BAR domain protein required for membrane invagination in CME (Wigge et al., 1997). Amphiphysin has a lipid interacting BAR (Bin–AMPH–Rvs) domain in its N-terminal, a medial clathrin/AP-2 binding (CLAP) domain and C-terminal Src homology 3 (SH3) domain. The BAR domain of amphiphysin forms crescent-shaped dimer and its concave surface serves as a platform for bending membrane or sensing membrane curvature (Peter et al., 2004). The CLAP domain binds to clathrin and AP-2, major components of clathrin coated pits, and helps to recruit amphiphysin to the sites of CME. In addition, the C-terminal SH3domain of amphiphysin binds directly to the PRD of dynamin 1 (David, McPherson, Mundigl, & de Camilli, 1996; Takei, Slepnev, Haucke, & De Camilli, 1999) and enhances dynamin's GTPase activity in the presence of liposomes (Takei et al., 1999; Yoshida et al., 2004). Amphiphysin copolymerizes with dynamin 1 into washer ring-shaped complexes, which form membrane tubules *in vitro* (Takei et al., 1999; Yoshida et al., 2004) similar to those formed from synaptic plasma membranes (Takei et al., 1995). Furthermore, injection of specific antibodies against amphiphysin into the giant synapse in lampreys (Evergren et al., 2004) or amphiphysin KO in mice (Di Paolo et al., 2002) causes suppressed endocytosis in synaptic vesicle recycling. These results suggest that dynamin mediates membrane fission in CME in collaboration with amphiphysin *in vivo*. However, precise contribution of amphiphysin in the dynamin-mediated membrane fission remains elusive.

In this study, we analyze dynamics of dynamin-amphiphysin ring complexes using a novel approach combining EM and HS-AFM. Firstly, we show that the dynamin-amphiphysin rings are rearranged to form clusters upon GTP hydrolysis, and membrane constriction occurs at protein-uncoated regions between the clusters. Secondly, we reveal that GTP hydrolysis is required and sufficient for the cluster formation by dynamin-amphiphysin complexes by EM analyses. Finally, we show a novel function of amphiphysin in controlling cluster size, which in turn regulates biogenesis of endocytic vesicles. These findings provide new insights into the mechanism of membrane constriction and fission by dynamin-amphiphysin complexes.

RESULTS

GTP hydrolysis is required and sufficient for membrane constriction by dynamin-amphiphysin complexes

To elucidate the mechanisms of dynamin-mediated membrane fission, we reconstituted the minimum system *in vitro* and analyzed the time course of its structural changes using EM. Human dynamin 1 and amphiphysin were purified (Figure 1-figure supplement 1A) and their activity to form ring-shaped complexes in a buffer of physiological ionic strength and pH condition was confirmed (Figure 1-figure supplement 1B). As previously described (Sweitzer & Hinshaw, 1998; Takei et al., 1998; Takei et al., 1999), the dynamin-amphiphysin complexes induced tubulation of large unilamellar vesicles (LUVs) in the absence of GTP (Figure 1A, No GTP). Immediately after the addition of 1 mM GTP, the appearance of lipid tubules was not affected (Figure 1A, GTP 1 s), but they started to form multiple constriction sites over time (Figure 1A, GTP 5 s, 10 s and 30 s) and membrane fission occurred finally and numerous vesicles were generated within 1 min (Figure 1A, GTP 1 min).

Next, we tried to clarify how the membrane constriction and fission by dynamin-amphiphysin ring complexes are correlated with guanine nucleotide conditions during GTP hydrolysis. The appearance of lipid tubules (Figure 1B, No GTP) was not affected in the presence of either slowly-hydrolyzable GTP analogue GTPγS (Figure 1B, GTPγS) or non-hydrolyzable GTP analogue GMP-PNP (guanosine 5′-[β,γ-imido]triphosphate) (Figure 1B, GMP-PNP). In contrast, in the presence of GDP (guanosine diphosphate) and vanadate, the complex which mimics the GDP · Pi transition state, lipid tubules were constricted at multiple sites (Figure 1B, GDP + vanadate). Addition of only GDP did not cause membrane constriction or fission, but membrane tubules were deformed (Figure 1B, GDP). Finally, numerous vesicles were generated 10 min after the addition of 1 mM GTP, in which multiple rounds of GTP hydrolysis were likely to have taken place (Figure 1B, GTP 10 min). Taken these results together, GTP hydrolysis is essential for both membrane constriction and fission by the dynamin-amphiphysin complexes, but subsequent dissociation of GTP hydrolytic products (GDP and/or phosphate) is required for completing membrane fission.

GTP hydrolysis induces clustering of dynamin-amphiphysin ring complexes

Although we determined the requirement of GTP hydrolysis in membrane constriction and fission by the dynamin-amphiphysin complexes, structural changes of the complexes were not clearly resolved in the *in vitro* assay system using LUVs. To improve the resolution, we used

rigid lipid nanotubes containing glycolipid galactosylceramide (GalCer) (Wilson-Kubalek, Brown, Celia, & Milligan, 1998), instead of using LUVs in the *in vitro* assay system. Lipid nanotubes are rod-shaped liposomes and similar in size to the unconstricted necks of clathrin-coated pits observed *in vivo* (Figure 2A, Nanotube). Dynamin-amphiphysin complexes assembled into helices on the lipid nanotubes (Figure 2A, No GTP), which is similar to those formed by dynamin alone (Stowell, Marks, Wigge, & McMahon, 1999). Interestingly, the dynamin-amphiphysin rings transiently formed clusters after the addition of GTP (Figure 2A, GTP 1 s and 20 s, brackets). The dynamin-amphiphysin clusters were disorganized over time and partially dissociated from the nanotubes (Figure 2A, GTP 30 s and 1 min).

To correlate the dynamics of dynamin-amphiphysin complexes with GTP hydrolysis, we examined structural changes of the complexes on lipid nanotubes at different transition states of GTP hydrolysis. The appearance of dynamin-amphiphysin helices was unchanged even in the presence of GTPγS or GMP-PNP (Figure 2B, No GTP, GTPγS and GMP-PNP). Interestingly, addition of GDP and vanadate induced rearrangement of the dynamin-amphiphysin ring complexes to form clusters similar to those observed after the addition of GTP (Figure 2B, GDP + vanadate). The average pitch between washer-rings in the clusters were shorter (15.00 nm ± 2.2, mean pitch ± s.e.m.) compared to the average pitch of the ring complexes in No GTP control (19.96 nm ± 0.47, mean pitch ± s.e.m.). In contrast, GDP alone did not affect the distribution of dynamin-amphiphysin rings (Figure 2B, GDP). Finally, the dynamin-amphiphysin ring complexes were disorganized and eventually dissociated from the lipid nanotubes 10 min after the addition of 1 mM GTP (Figure 2B, GTP 10 min). Taken these results together, the dynamin-amphiphysin ring complexes transiently form clusters in the GTP hydrolysis transition state of GDP · Pi during which membrane tubules are constricted.

HS-AFM revealed dynamic clustering of dynamin-amphiphysin ring complexes upon GTP hydrolysis

To elucidate the dynamics of dynamin-amphiphysin ring complexes during the membrane constriction and fission, we analyzed the clustering process of the complexes using HS-AFM (Ando, Uchihashi, & Kodera, 2013). LUVs were stably immobilized on the carbon-coated and glow-discharged mica substrate (Figure 3-figure supplement 1A; Supplementary Movie S1), and they were successfully tubulated in the presence of dynamin and amphiphysin (Figure 3-figure supplement 1B; Supplementary Movie S2). The dynamin-amphiphysin rings on the lipid tubules were aligned with an almost regular pitch (22.04 nm ± 0.68, mean pitch ± s.e.m.) and they were

immobile before GTP addition (Figure 3A, 0 s and 21 s; Supplementary Movie S3). Interestingly, the dynamin-amphiphysin rings became mobile after GTP addition and eventually formed clusters consisting of a few rings with shorter pitch (15.72 nm ± 0.30, mean pitch ± s.e.m.) (Figure 3A, from 42 s to 131 s; Supplementary Movie S3). Particle tracking analyses of the individual dynamin-amphiphysin rings showed that the dynamin-amphiphysin complexes were static before GTP addition (Figure 3B, 5-21 sec; Supplementary Movie S4), but addition of 1mM GTP stimulated longitudinal movement of the ring complexes, leading to the cluster formation (Figure 3B, 38-54 sec, 38-86 sec and 38-118 sec; Supplementary Movie S5). Although membrane fission was not observed in this sample probably due to a strong attachment of the lipid tubule to the substrate, the rings had a tendency to constrict during cluster formation (Figure 3C; Figure 3-figure supplement 2). These results suggest that dynamin-amphiphysin ring complexes undergo two modes of structural changes, longitudinal clustering and radial constriction, during GTP hydrolysis.

Membrane fission occurs at protein-uncoated regions flanking dynamin-amphiphysin clusters

We next tried to correlate the cluster formation of dynamin-amphiphysin ring complexes with membrane constriction and fission. In the representative sample in which membrane constriction and fission occurred, a few dynamin-amphiphysin rings merged to form a cluster over time after GTP addition (Figure 4A, 0 s, 125.3 s, 185.5 s and 227.5 s; Supplementary Movie S6). Interestingly, membrane constriction occurred at flanking regions of the cluster where membrane was bare of dynamin-amphiphysin complexes (Figure 4A, fission point (FP).1 and FP.2). The heights at sites marked with FP.1 and FP.2 were not changed before constriction (Figure 4B, before constriction), but they became lower in a stepwise manner from a pre-constriction height of around 30 nm down to 20-25 nm or below (Figure 4B, after constriction). Similar longitudinal redistribution of the dynamin-amphiphysin rings before membrane constriction was also observed in another sample, in which constriction occurred at one end of clustered dynamin-amphiphysin complexes (Figure.4c, arrow；Supplementary Movie S8). These results strongly suggest that membrane constriction and fission occur at the protein-uncoated regions created as a result of the clustering of dynamin-amphiphysin ring complexes.

Amphiphysin contributes to efficient vesicle formation by controlling cluster formation

We previously demonstrated that amphiphysin stimulates the GTPase activity of dynamin and thus enhances vesicle biogenesis (Yoshida et al., 2004). In this study, we also noticed that the

average size of vesicles formed by dynamin-amphiphysin complexes (69.99 ± 2.93 nm, mean diameter ± s.e.m.) was significantly smaller compared to those formed by dynamin alone (204.58 ± 12.25 nm, mean diameter ± s.e.m.) after GTP addition (Figure 5A). Consistently, dynamin-amphiphysin complex formed constriction sites with shorter intervals (150.28 ± 9.75 nm, mean intervals ± s.e.m.) compared to those formed by dynamin alone (193.49 ± 15.82 nm, mean intervals ± s.e.m.) in the presence of GDP and vanadate (Figure 5B). To further elucidate roles of amphiphysin in the membrane constriction and fission, the cluster formation by dynamin alone was compared to that by dynamin-amphiphysin complexes, using lipid nanotubes. As already described, dynamin-amphiphysin complexes formed clusters with a few rings in the presence of GDP and vanadate (34.22 ± 1.66 nm, mean cluster size ± s.e.m.) (Figure 5C, Dynamin + Amphiphysin). In contrast, dynamin alone formed larger-sized clusters consist of more ring complexes (59.27 ± 4.69 nm, mean cluster size ± s.e.m.) (Figure 5C, Dynamin). These results suggest that amphiphysin contributes to the effective generation of properly sized vesicles by controlling the cluster formation of dynamin-amphiphysin ring complexes.

DISCUSSION

In this study, we analyzed dynamics of dynamin-amphiphysin ring complexes during membrane constriction and fission using EM and HS-AFM. EM analyses showed that GTP hydrolysis is required for both membrane constriction and fission, but dissociation of hydrolytic products (GDP and/or phosphate) seems necessary for the completion of membrane fission (Figure 1). In the presence of GTP or GDP and vanadate, dynamin-amphiphysin ring complexes are reorganized, resulting in the formation of clusters consisting of a few dynamin-amphiphysin rings (Figure 2). HS-AFM analyses directly demonstrated that GTP hydrolysis induces dynamic longitudinal movement of the dynamin-amphiphysin rings as well as constriction during cluster formation (Figure 3). Interestingly, HS-AFM analyses also demonstrated that membrane constriction and fission occur at the "protein-uncoated" regions created as a result of cluster formation of dynamin-amphiphysin complexes (Figure 4). Finally, we found that amphiphysin contributes to effective biogenesis of endocytic vesicles by regulating size of the clusters formed by dynamin-amphiphysin ring complexes (Figure 5).

There is a consensus view about the requirement of GTP hydrolysis in membrane fission, but the requirement of GTP hydrolysis in membrane constriction is still controversial (Antonny et al., 2016). Membrane tubules are constricted in the presence of non-hydrolyzable GTP analogue (Chen et al., 2004; Mears et al., 2007; Zhang & Hinshaw, 2001) and more constricted with a GTP-loaded GTPase defective K44A mutant (Sundborger et al., 2014). In both cases, membrane tubules are evenly constricted and periodical membrane constriction sites which lead to membrane fission is not created. In the present study, we showed that membrane constriction sites are created in the presence of GDP and vanadate, which mimicked a transition state of GTP hydrolysis (GDP · Pi), suggesting that complete hydrolysis of GTP is required for the formation of constriction sites leading to membrane fission (Figure 1B). Membrane fission has never been observed in the presence of GDP and vanadate, suggesting that release of GTP hydrolytic products (GDP and/or phosphate) is a prerequisite for membrane fission. Further analyses will more precisely reveal which intermediate state in the GTPase reaction is responsible for the membrane fission or how many GTPase cycles are required for it.

In this study, we revealed that dynamin-amphiphysin ring complexes are rearranged to form their clusters upon GTP hydrolysis (Figure 2 and Figure 3) and membrane fission occurs at the flanking "protein-uncoated" membrane regions (Figure 4). In the "constrictase" model, dynamin constricts membrane until the membrane neck reaches to the hemi-fission state, which leads to spontaneous membrane fission (Chen et al., 2004; Hinshaw & Schmid, 1995; Mears et al., 2007).

However, several lines of evidences are apparently inconsistent with this simple model. For instance, the super-constricted state of dynamin does not constrict the membrane sufficiently enough to reach the hemi-fission state (Sundborger et al., 2014) and membrane tension and/or torsion is required to overcome the energy barrier to fission (Bashkirov et al., 2008; Morlot et al., 2012; Roux et al., 2006). Based on these results and our results in this study, we propose a novel model of membrane fission by dynamin-amphiphysin complexes, for which we term "clusterase" model (Figure 6). First, dynamin-amphiphysin are assembled to form washer ring-like or helical polymers to induce membrane tubulation (Figure 6A). GTP hydrolysis induces dynamic longitudinal rearrangement of dynamin-amphiphysin rings to form clusters (Figure 6B). The clustered dynamin-amphiphysin rings also constrict to give local tension and/or torsion to the membrane tube at the edge of the clusters (Figure 6C). Alternatively, the dynamin-amphiphysin clusters may serve as a lipid diffusion barrier that causes friction leading to membrane scission (Simunovic et al., 2017). Finally, membrane fission occurs along with disassembly of the dynamin-amphiphysin polymers into oligomers (Figure 6D). Longitudinal rearrangement upon GTP hydrolysis similar to the cluster formation by the dynamin-amphiphysin complexes was also observed in an EM study on the dynamics of dynamin with lipid nanotubes (Stowell et al., 1999) and more recently by HS-AFM analyses on dynamics of ΔPRD dynamin (Colom, Redondo-Morata, Chiaruttini, Roux, & Scheuring, 2017), suggesting that the longitudinal rearrangement is an intrinsic property of dynamin during membrane fission.

We revealed that amphiphysin possibly contributes to effective vesicle biogenesis by controlling the number of constriction sites in a long membrane tubule formed *in vitro* (Figure 5).Ttubular structures have long been known to be present in various synapses, and they are described as "membrane tubules" (J. Heuser & Miledi, 1971) , "cisternae" (J. E. Heuser & Reese, 1973), "synaptic tubules" (Samorajski, Ordy, & Keefe, 1966) or "anastomosing tubules" (Ekstrom von Lubitz, 1981). The tubules are enriched in endocytic proteins including dynamin, synaptojanin, amphiphysin, and endophilin (Fuchs, Brandstatter, & Regus-Leidig, 2014; Takei et al., 1998), and the presence of the tubules becomes more prominent when synapses are stimulated (Fuchs et al., 2014; Takei et al., 1998), or when membrane fission is blocked in dynamin 1 K.O. mice (Ferguson et al., 2007). These findings strongly suggest that the tubular structures represent endocytic intermediate at which dynamin-amphiphysin-dependent synergic vesicle formation takes place in the synapse. Besides amphiphysin, other BAR domain proteins, endophilin and syndapin, are also implicated in synaptic vesicle recycling (Dittman & Ryan,

2009; Koch et al., 2011; Milosevic et al., 2011). One of the important future goals of dynamin study would be to clarify regulatory mechanisms by which dynamin alters its interactions with various BAR proteins during synaptic vesicle recycling process.

In conclusion, live imaging analyses using HS-AFM in this study and a study from another group (Colom et al., 2017) gave new mechanistic insights into the dynamin-mediated membrane fission. Combinatory approaches using high temporal resolution imaging with HS-AFM and high spatial resolution structural analyses with X-ray crystallography or Cryo-EM will be the most powerful approach in resolving various dynamic membrane remodeling processes in the future.

MATERIALS AND METHODS

Purification of dynamin1 and amphiphysin

Human dynamin1 was purified using the method of Warnock et al with some modification (Warnock, Hinshaw, & Schmid, 1996). Sf9 cells grown in 600 ml of SF-900II SFM (Life Technologies) to the cell density of 1×10^6 cells/ml and the cells were infected with baculoviruses expressing dynamin1. After cultivation of cells at 28 ℃for 69 hours, the infected Sf9 cells were harvested by centrifugation at 500 × g for 10 min. The cell pellet was resuspended by 1/20 of the culture volume (30 ml) of HCB (Hepes column buffer)100 (20 mM Hepes, 100 mM NaCl, 2 mM EGTA, 1 mM $MgCl_2$, 1 mM DTT, 1 mM PMSF, 1 μg/ml Pepstatin A, 40 μM ALLN, pH 7.2) and cells were sonicated using a sonicator (Advanced-Digital SONIFIER model 250, BRANSON). The cell lysate was mixed with equal volume of HCB0 (20 mM Hepes, 2 mM EGTA, 1 mM $MgCl_2$, 1 mM DTT, 1 mM PMSF, 1 μg/ml Pepstatin A, 40 μM ALLN, pH 7.2) to make HCB50 (20 mM Hepes, 50 mM NaCl, 2 mM EGTA, 1 mM $MgCl_2$, 1 mM DTT, 1 mM PMSF, 1 μg/ml Pepstatin A, 40 μM ALLN, pH7.2) and centrifuged at 210,000 × g for 1h at 4℃. Ammonium sulfate was added to the cleared lysate to the 30% saturation and incubated at 4℃ for 30min and centrifuged at 10,000 × g for 10min to recover the dynamin1 containing fraction in the pellet. The dynamin1 pellet was resuspended with 20 ml of HCB50 and dialyzed against 2L of HCB50 for total 4 hours (2 hours, 2 times) using dialysis membrane (Spectra/Por®Dialysis Membrane MWCO: 3500). The dialyzed dynamin1 fraction was applied to Mono Q5/50GL column (GE healthcare) and bound proteins were eluted stepwise using HCB50, HCB100, HCB250 and HCB1000 buffers. Purified dynamin1 was recovered in HCB250 fraction and purity was determined by SDS-PAGE (Figure 1-figure supplement 1A, Dynamin).

Human amphiphysin was purified following manufacture's instruction (GE Healthcare) with slight modifications. Host bacteria BL21 (DE3) transformed with an expression construct for GST fusions of human amphiphysin (pGEX6P2-HsAMPH) were grown in 1 L of LB medium to the cell density of 0.6-0.8 (OD 600 nm) at 37 ℃ and then protein expression was induced at 18 ℃ for 12 hours in the presence of 0.1 mM IPTG. The bacterial cells were harvested by centrifugation at 7,000 × g for 10 min and cell pellet was resuspended by 1/10 culture volume (100 ml) of Elution/Wash 300 buffer (50 mM Tris-HCl, pH 8.0, 300 mM NaCl). The resuspended cells were sonicated using Advanced-Digital SONIFIER model 250D (Branson) and centrifuged at 261,000 × g for 30 min at 4 ℃ and cleared lysate was recovered in supernatant. To the cleared lysate, 1/100 culture volume (1 ml in bed volume) of Glutathione

Sepharose 4B Beads (GE Healthcare) was added and they are mixed using rotating mixer for 1h at 4℃. The beads were washed with the Elution/Wash 300 buffer for 5 times in a repeated cycle of centrifugation at 420 × g for 5 min at 4 ℃ followed by mixing with rotator for 5 min at 4℃. The beads with purified GST fusions of amphiphsyin were equilibrated with PreScission Buffer (50 mM Tris-HCl, 150 mM NaCl, 1 mM EDTA, 1 mM DTT, pH 7.0) and GST-tag was removed by PreScission Protease (GE Healthcare) by incubating for 12 h at 4 ℃. The purified amphiphysin was recovered by centrifuge (12,000 × g, 5 min at 4 ℃) using spin column (Ultrafree-Mc, GV 0.22 μm, Millipore) and purity was determined by SDS-PAGE (Figure 1-figure supplement 1A, Amphiphysin).

Preparation of LUVs and lipid nanotubes

Large unilamellar vesicles (LUVs) and lipid nanotubes were prepared as previously described (Takei, Slepnev, & De Camilli, 2001). For LUVs, 70% PS (Cat. No 840032C, Avanti), 10% biotinPE (Avanti) and 10 % cholesterol (Avanti) were mixed and, for lipid nanotubes 40% NFA Galactocerebrosides (Sigma C1516), 40% PC (Avanti), 10% PI(4,5)P_2 (Calbiochem) and 10% cholesterol (Avanti) were mixed in 250 μl of chloroform in a glass vial (Mighty Vial No.01 4 ml, Maruemu Cat. No 5-115-03). Then chloroform was evaporated using slow-flow nitrogen gas to produce lipid a lipid film on the glass and then completely dried in a vacuum desiccator for 30min. The dried lipid was rehydrated by water-saturated nitrogen gas followed by addition of 250 μl of filtered 0.3M sucrose for 2h at 37 ℃. The resultant LUVs and lipid nanotubes were passed through 0.4 μm- and 0.2 μm- polycarbonate filters respectively 11 times using Avanti Mini extruder. The LUVs and lipid nanotubes (1 mg/ml of final concentration) were stored in dark at 4 ℃ avoiding photooxidation.

EM imaging of in vitro assay with liposomes and dynamin-amphiphysin complexes

LUVs and lipid nanotubes were diluted to 0.17 mg/ml in cytosolic buffer (25 mM Hepes-KOH, pH 7.2, 25 mM KCl, 2.5 mM Magnesium acetate, 0.1 M K-glutamate, pH 7.4). Dynamin-amphiphysin complexes (1:1 in molar ratio) were diluted to 0.6 μM in the cytosolic buffer. Formvar filmed EM grids were carbon-coated, then glow-discharged. Droplets of the diluted lipids (10μl each) were prepared on Parafilm and adsorbed on EM grids for 5 min at room temperature. Then the EM grids with lipids were transferred to other droplets of the diluted dynamin-amphiphysin complexes and incubated for 30 min at room temperature in a humid chamber. To see the temporal effect of GTP hydrolysis, the EM grids were transferred to

1mM of GTP and incubated for various time periods (from 1s to 10 min) at room temperature. Alternatively, the EM grids were incubated either GTP, GTPγS, GMP-PNP, GDP plus Vanadate and GDP to analyze GTP hydrolysis transition state structures. The EM grids were negatively stained with filtered 2% uranyl acetate and observed with transmission electron microscope (HITACHI H-7650).

HS-AFM imaging

All AFM images shown in this article were capture by a laboratory-built HS-AFM in which the amplitude-modulation mode was used. For the HS-AFM imaging, a small cantilever with dimensions of 7-μm long, 2-μm wide, and 90-nm thick was used (Olympus). Its nominal spring constant and resonant frequency were ~0.1 N/m and ~800 kHz in an aqueous solution, respectively. To obtain a sharp tip, an amorphous carbon pillar was grown on the original bird-beak tip of the cantilever by electron beam deposition (EBD) and then sharpened by a plasma etching in an argon environment. The typical radius of the EBD tip was approximately 2 nm after sharpening. For the amplitude-modulation imaging, the cantilever was oscillated with amplitude less than 10 nm under free oscillation condition and the set-point was set at ~90% of the free oscillation amplitude. For HS-AFM imaging of liposomes and dynamin-amphiphysin complexes with lipid tubules or nanotubes, we used mica covered with carbon film. After coating a freshly cleaved mica surface with carbon film, hydrophilic treatment was carried out by a grow discharge. The liposomes (0.17 mg/ml) were deposited on the hydrophilic mica surface and incubated for 5 min at room temperature followed by deposition of proteins (0.6 μM of dynamin1 and amphiphysin) for 30 min at room temperature. After the incubation, the sample was thoroughly washed by cytosolic buffer to remove excess liposomes and proteins. After the washing, the cantilever tip was approached and the imaging was performed under the buffer.

Quantitative data analyses of EM and HS-AFM images

The EM and HS-AFM images were randomly captured to avoid data manipulation and representative images were shown in all the figures. The average pitch between the dynamin-amphiphysin washer rings in EM images (Figure 2) and HS-AFM images (Figure 3), diameter of vesicles, intervals between constriction sites and size of clusters generated by either dynamin-amphiphysin complex or dynamin (Figure 5), were all measured by FIJI (Schindelin et

al., 2012). Experimental data was statistically analyzed using Excel (Microsoft) or Prism 7 (GraphPad software).

ACKNOWLEDGEMENTS

The authors thank Dr. Aurélien Roux and Dr. Adai Colom (University of Geneva), Dr. Lorena Redondo-Morata (INSERM U1006/Aix-Marseille Université) and Dr. Masatoshi Ichikawa (Kyoto University) for their critical reading of the manuscript. This work was supported by JST/CREST program (#JPMJCR13M1) (to T.A. and K.T.). This work was also supported in part by JSPS KAKENHI Grant Numbers JP15H03540 (to T.U.), MEXT KAKENHI Grant Numbers JP16H00830 and JP16H00758 (to T.U.).

COMPETING INTERESTS

No competing interests declared.

REFERENCES

Ando, T., Uchihashi, T., & Kodera, N. (2013). High-speed AFM and applications to biomolecular systems. *Annu Rev Biophys, 42*, 393-414. doi:10.1146/annurev-biophys-083012-130324

Antonny, B., Burd, C., De Camilli, P., Chen, E., Daumke, O., Faelber, K., . . . Schmid, S. (2016). Membrane fission by dynamin: what we know and what we need to know. *EMBO J, 35*(21), 2270-2284. doi:10.15252/embj.201694613

Bashkirov, P. V., Akimov, S. A., Evseev, A. I., Schmid, S. L., Zimmerberg, J., & Frolov, V. A. (2008). GTPase cycle of dynamin is coupled to membrane squeeze and release, leading to spontaneous fission. *Cell, 135*(7), 1276-1286. doi:10.1016/j.cell.2008.11.028

Cao, H., Garcia, F., & McNiven, M. A. (1998). Differential distribution of dynamin isoforms in mammalian cells. *Mol Biol Cell, 9*(9), 2595-2609.

Chen, Y. J., Zhang, P., Egelman, E. H., & Hinshaw, J. E. (2004). The stalk region of dynamin drives the constriction of dynamin tubes. *Nat Struct Mol Biol, 11*(6), 574-575. doi:10.1038/nsmb762

Cocucci, E., Gaudin, R., & Kirchhausen, T. (2014). Dynamin recruitment and membrane scission at the neck of a clathrin-coated pit. *Mol Biol Cell, 25*(22), 3595-3609. doi:10.1091/mbc.E14-07-1240

Colom, A., Redondo-Morata, L., Chiaruttini, N., Roux, A., & Scheuring, S. (2017). Dynamic remodeling of the dynamin helix during membrane constriction. *Proc Natl Acad Sci U S A, 114*(21), 5449-5454. doi:10.1073/pnas.1619578114

Cook, T., Mesa, K., & Urrutia, R. (1996). Three dynamin-encoding genes are differentially expressed in developing rat brain. *J Neurochem, 67*(3), 927-931.

Cook, T. A., Urrutia, R., & McNiven, M. A. (1994). Identification of dynamin 2, an isoform ubiquitously expressed in rat tissues. *Proc Natl Acad Sci U S A, 91*(2), 644-648.

David, C., McPherson, P. S., Mundigl, O., & de Camilli, P. (1996). A role of amphiphysin in synaptic vesicle endocytosis suggested by its binding to dynamin in nerve terminals. *Proc Natl Acad Sci U S A, 93*(1), 331-335.

Di Paolo, G., Sankaranarayanan, S., Wenk, M. R., Daniell, L., Perucco, E., Caldarone, B. J., . . . De Camilli, P. (2002). Decreased synaptic vesicle recycling efficiency and cognitive deficits in amphiphysin 1 knockout mice. *Neuron, 33*(5), 789-804.

Dittman, J., & Ryan, T. A. (2009). Molecular circuitry of endocytosis at nerve terminals. *Annu Rev Cell Dev Biol, 25*, 133-160. doi:10.1146/annurev.cellbio.042308.113302

Ekstrom von Lubitz, D. K. (1981). Ultrastructure of the lateral-line sense organs of the ratfish, Chimaera monstrosa. *Cell Tissue Res, 215*(3), 651-665.

Evergren, E., Marcucci, M., Tomilin, N., Low, P., Slepnev, V., Andersson, F., . . . Shupliakov, O. (2004). Amphiphysin is a component of clathrin coats formed during synaptic vesicle recycling at the lamprey giant synapse. *Traffic, 5*(7), 514-528. doi:10.1111/j.1398-9219.2004.00198.x

Faelber, K., Held, M., Gao, S., Posor, Y., Haucke, V., Noe, F., & Daumke, O. (2012). Structural insights into dynamin-mediated membrane fission. *Structure, 20*(10), 1621-1628. doi:10.1016/j.str.2012.08.028

Faelber, K., Posor, Y., Gao, S., Held, M., Roske, Y., Schulze, D., . . . Daumke, O. (2011). Crystal structure of nucleotide-free dynamin. *Nature, 477*(7366), 556-560. doi:10.1038/nature10369

Ferguson, S. M., Brasnjo, G., Hayashi, M., Wolfel, M., Collesi, C., Giovedi, S., . . . De Camilli, P. (2007). A selective activity-dependent requirement for dynamin 1 in synaptic vesicle endocytosis. *Science, 316*(5824), 570-574. doi:10.1126/science.1140621

Ferguson, S. M., & De Camilli, P. (2012). Dynamin, a membrane-remodelling GTPase. *Nat Rev Mol Cell Biol, 13*(2), 75-88. doi:10.1038/nrm3266

Ford, M. G., Jenni, S., & Nunnari, J. (2011). The crystal structure of dynamin. *Nature, 477*(7366), 561-566. doi:10.1038/nature10441

Fuchs, M., Brandstatter, J. H., & Regus-Leidig, H. (2014). Evidence for a Clathrin-independent mode of endocytosis at a continuously active sensory synapse. *Front Cell Neurosci, 8*, 60. doi:10.3389/fncel.2014.00060

Heuser, J., & Miledi, R. (1971). Effects of lanthanum ions on function and structure of frog neuromuscular junctions. *Proc R Soc Lond B Biol Sci, 179*(1056), 247-260.

Heuser, J. E., & Reese, T. S. (1973). Evidence for recycling of synaptic vesicle membrane during transmitter release at the frog neuromuscular junction. *J Cell Biol, 57*(2), 315-344.

Hinshaw, J. E., & Schmid, S. L. (1995). Dynamin self-assembles into rings suggesting a mechanism for coated vesicle budding. *Nature, 374*(6518), 190-192. doi:10.1038/374190a0

Kirchhausen, T., Owen, D., & Harrison, S. C. (2014). Molecular structure, function, and dynamics of clathrin-mediated membrane traffic. *Cold Spring Harb Perspect Biol, 6*(5), a016725. doi:10.1101/cshperspect.a016725

Koch, D., Spiwoks-Becker, I., Sabanov, V., Sinning, A., Dugladze, T., Stellmacher, A., . . . Qualmann, B. (2011). Proper synaptic vesicle formation and neuronal network activity critically rely on syndapin I. *EMBO J, 30*(24), 4955-4969. doi:10.1038/emboj.2011.339

Koenig, J. H., & Ikeda, K. (1989). Disappearance and reformation of synaptic vesicle membrane upon transmitter release observed under reversible blockage of membrane retrieval. *J Neurosci, 9*(11), 3844-3860.

Marks, B., Stowell, M. H., Vallis, Y., Mills, I. G., Gibson, A., Hopkins, C. R., & McMahon, H. T. (2001). GTPase activity of dynamin and resulting conformation change are essential for endocytosis. *Nature, 410*(6825), 231-235. doi:10.1038/35065645

Mattila, J. P., Shnyrova, A. V., Sundborger, A. C., Hortelano, E. R., Fuhrmans, M., Neumann, S., . . . Frolov, V. A. (2015). A hemi-fission intermediate links two mechanistically distinct stages of membrane fission. *Nature, 524*(7563), 109-113. doi:10.1038/nature14509

McMahon, H. T., & Boucrot, E. (2011). Molecular mechanism and physiological functions of clathrin-mediated endocytosis. *Nat Rev Mol Cell Biol, 12*(8), 517-533. doi:10.1038/nrm3151

Mears, J. A., Ray, P., & Hinshaw, J. E. (2007). A corkscrew model for dynamin constriction. *Structure, 15*(10), 1190-1202. doi:10.1016/j.str.2007.08.012

Milosevic, I., Giovedi, S., Lou, X., Raimondi, A., Collesi, C., Shen, H., . . . De Camilli, P. (2011). Recruitment of endophilin to clathrin-coated pit necks is required for efficient vesicle uncoating after fission. *Neuron, 72*(4), 587-601. doi:10.1016/j.neuron.2011.08.029

Morlot, S., Galli, V., Klein, M., Chiaruttini, N., Manzi, J., Humbert, F., . . . Roux, A. (2012). Membrane shape at the edge of the dynamin helix sets location and duration of the fission reaction. *Cell, 151*(3), 619-629. doi:10.1016/j.cell.2012.09.017

Peter, B. J., Kent, H. M., Mills, I. G., Vallis, Y., Butler, P. J., Evans, P. R., & McMahon, H. T. (2004). BAR domains as sensors of membrane curvature: the amphiphysin BAR structure. *Science, 303*(5657), 495-499. doi:10.1126/science.1092586

Reubold, T. F., Faelber, K., Plattner, N., Posor, Y., Ketel, K., Curth, U., . . . Eschenburg, S. (2015). Crystal structure of the dynamin tetramer. *Nature, 525*(7569), 404-408. doi:10.1038/nature14880

Roux, A., Uyhazi, K., Frost, A., & De Camilli, P. (2006). GTP-dependent twisting of dynamin implicates constriction and tension in membrane fission. *Nature, 441*(7092), 528-531.

doi:10.1038/nature04718

Samorajski, T., Ordy, J. M., & Keefe, J. R. (1966). Structural organization of the retina in the tree shrew (Tupaia glis). *J Cell Biol, 28*(3), 489-504.

Schindelin, J., Arganda-Carreras, I., Frise, E., Kaynig, V., Longair, M., Pietzsch, T., . . . Cardona, A. (2012). Fiji: an open-source platform for biological-image analysis. *Nat Methods, 9*(7), 676-682. doi:10.1038/nmeth.2019

Schmid, S. L., & Frolov, V. A. (2011). Dynamin: functional design of a membrane fission catalyst. *Annu Rev Cell Dev Biol, 27*, 79-105. doi:10.1146/annurev-cellbio-100109-104016

Simunovic, M., Manneville, J. B., Renard, H. F., Evergren, E., Raghunathan, K., Bhatia, D., . . . Callan-Jones, A. (2017). Friction Mediates Scission of Tubular Membranes Scaffolded by BAR Proteins. *Cell, 170*(1), 172-184 e111. doi:10.1016/j.cell.2017.05.047

Stowell, M. H., Marks, B., Wigge, P., & McMahon, H. T. (1999). Nucleotide-dependent conformational changes in dynamin: evidence for a mechanochemical molecular spring. *Nat Cell Biol, 1*(1), 27-32. doi:10.1038/8997

Sundborger, A. C., Fang, S., Heymann, J. A., Ray, P., Chappie, J. S., & Hinshaw, J. E. (2014). A dynamin mutant defines a superconstricted prefission state. *Cell Rep, 8*(3), 734-742. doi:10.1016/j.celrep.2014.06.054

Sweitzer, S. M., & Hinshaw, J. E. (1998). Dynamin undergoes a GTP-dependent conformational change causing vesiculation. *Cell, 93*(6), 1021-1029.

Takei, K., Haucke, V., Slepnev, V., Farsad, K., Salazar, M., Chen, H., & De Camilli, P. (1998). Generation of coated intermediates of clathrin-mediated endocytosis on protein-free liposomes. *Cell, 94*(1), 131-141.

Takei, K., McPherson, P. S., Schmid, S. L., & De Camilli, P. (1995). Tubular membrane invaginations coated by dynamin rings are induced by GTP-gamma S in nerve terminals. *Nature, 374*(6518), 186-190. doi:10.1038/374186a0

Takei, K., Slepnev, V. I., & De Camilli, P. (2001). Interactions of dynamin and amphiphysin with liposomes. *Methods Enzymol, 329*, 478-486.

Takei, K., Slepnev, V. I., Haucke, V., & De Camilli, P. (1999). Functional partnership between amphiphysin and dynamin in clathrin-mediated endocytosis. *Nat Cell Biol, 1*(1), 33-39. doi:10.1038/9004

Warnock, D. E., Hinshaw, J. E., & Schmid, S. L. (1996). Dynamin self-assembly stimulates its GTPase activity. *J Biol Chem, 271*(37), 22310-22314.

Wigge, P., Kohler, K., Vallis, Y., Doyle, C. A., Owen, D., Hunt, S. P., & McMahon, H. T. (1997). Amphiphysin heterodimers: potential role in clathrin-mediated endocytosis. *Mol Biol Cell, 8*(10), 2003-2015.

Wilson-Kubalek, E. M., Brown, R. E., Celia, H., & Milligan, R. A. (1998). Lipid nanotubes as substrates for helical crystallization of macromolecules. *Proc Natl Acad Sci U S A, 95*(14), 8040-8045.

Yoshida, Y., Kinuta, M., Abe, T., Liang, S., Araki, K., Cremona, O., . . . Takei, K. (2004). The stimulatory action of amphiphysin on dynamin function is dependent on lipid bilayer curvature. *EMBO J, 23*(17), 3483-3491. doi:10.1038/sj.emboj.7600355

Zhang, P., & Hinshaw, J. E. (2001). Three-dimensional reconstruction of dynamin in the constricted state. *Nat Cell Biol, 3*(10), 922-926. doi:10.1038/ncb1001-922

FIGURE LEGENDS

Figure 1. GTP hydrolysis is required and sufficient for membrane constriction by dynamin-amphiphysin ring complexes (A) Electron micrographs of lipid tubules induced by dynamin-amphiphysin ring complex before GTP addition (No GTP) and at different time points after addition of 1 mM GTP (GTP 1 s, GTP 5 s, GTP 10 s, GTP 30 s and GTP 1 min). More than thirty samples from three individual experiments were examined and representative images are shown. Scale bar is 200 nm. (B) Electron micrographs of lipid tubules induced by dynamin-amphiphysin ring complex without guanine nucleotide (No GTP) or with a transition states analogue of GTPase reaction, by adding 1 mM each of slowly hydrolyzable GTP analogue (GTPγS), nonhydrolyzable GTP analogue (GMP-PNP), GDP combined with vanadate (GDP + vanadate), GDP (GDP), or GTP (GTP) for 10 min. More than thirty samples from three individual experiments were examined and representative images are shown. Scale bar is 200 nm.

Figure 1-figure Supplement 1. Purified dynamin and amphiphysin forms ring-shaped complexes (A) SDS-PAGE of purified dynamin (Dynamin) and amphiphysin (Amphiphysin). (B) Negative staining electron micrographs of dynamin alone (Dynamin), dynamin and amphiphysin (Dynamin + Amphiphysin) and amphiphysin alone (Amphiphysin) incubated in cytosolic buffer with physiological salt concentration and PH (see materials and methods). Scale bar is 100 nm.

Figure 2. GTP hydrolysis induces clustering of dynamin-amphiphysin complexes on lipid nanotubes (A) Electron micrographs of a lipid nanotube (Nanotube) and those with dynamin-amphiphysin complexes before GTP addition (No GTP) and at different time points after GTP addition (GTP 1 s, GTP 20 s, GTP 30 s, and GTP 1 min). Clusters of dynamin-amphiphysin ring complexes are indicated (white brackets). More than thirty samples from three individual experiments were examined and representative images are shown. Scale bar is 100 nm. (B) Electron micrographs of lipid nanotubes after addition of dynamin-amphiphysin complexes without guanine nucleotide (No GTP) or with a transition states analogue of GTPase reaction, by adding 1 mM each of slowly hydrolysable GTP analogue (GTPγS), nonhydrolyzable GTP analogue (GMP-PNP), GDP combined with vanadate (GDP + vanadate), GDP (GDP) and GTP (GTP) for 10 min. More than thirty samples from three individual experiments were examined and representative images are shown. Clusters of dynamin-amphiphysin ring complexes are indicated (white brackets). The average pitch of washer-rings in the clusters is

15.00 ± 2.2 nm (mean pitch ± s.e.m., n=63 from 7 nanotubes) in GDP + vanadate, while the average pitch of the ring complexes is 19.96 ± 0.47 nm (mean pitch ± s.e.m., n=81 from 9 nanotubes) in No GTP control. Scale bar is 100 nm.

Figure 3. Dynamic clustering of dynamin-amphiphysin rings during GTP hydrolysis (A) HS-AFM images captured at 1 frame/s of dynamin-amphiphysin ring complexes on membrane tubules before (0 s and 21 s) and after GTP addition at different time points (42 s, 63 s, 84 s, 100 s, 115 s and 131 s). Dynamin-amphiphysin rings (arrowheads) are assembled into three distinct clusters (1, 2 and 3 at 131 s). The pitch of dynamin-amphiphysin rings on the lipid tubule was 22.04 ± 0.68 nm (mean pitch ± s.e.m., n=36 from 3 time points) before GTP addition and 15.72 ± 0.30 nm (mean pitch ± s.e.m., n=36 from 9 time points) after GTP addition. (B) Particle tracking of dynamin-amphiphysin rings before (5-21 sec) and after addition of 1mM GTP (38-54 sec, 38-86 sec and 38-118 sec) from Supplementary Movie S4 and S5, respectively. Particle tracking of the complexes in the cluster 2 (light blue, dark blue and magenta) and cluster 3 (red, yellow and green) are shown. (C) Dynamin-amphiphysin rings tend to constrict during clustering. Average heights before ($0 \leq t \leq 100$ sec) and after clustering (101 sec $\leq t$) are 38.38 ± 0.17 nm and 36.48 ± 0.18 nm for cluster 1, 32.62 ± 0.15 nm and 32.56 ± 0.18 nm for cluster 2, 27.90 ± 0.13 nm and 26.75 ± 0.18 nm for cluster 3, respectively. The heights were measured from the substrate surface. The marks *** indicate $p < 0.001$ and n.s. is not significant, respectively.

Figure 3-figure Supplement 1. HS-AFM imaging of LUV and its tubulation by dynamin-amphiphysin complex (A) HS-AFM images of a LUV. Scale bar is 50 nm. (B) Lipid tubules induced from LUVs in the presence of dynamin-amphiphysin complexes. Scale bar is 200 nm.

Figure 3-figure Supplement 2. Dynaimin-amphiphysin rings constrict during cluster formation Maximum heights of each rings plotted as a function of time (left panels) and their average ring heights before (0-100sec) and after clustering (101sec-) are shown for cluster1, 2 and 3 (A, B and C, respectively). ***: $p<0.001$, **: $p<0.01$, *: $p<0.1$, n.s.: not significant.

Figure 4. Membrane fission occurs at the protein-uncoated regions flanking dynamin-amphiphysin clusters (A) Clips of HS-AFM images captured at 0.42 frames/s showing membrane fission by dynamin-amphiphysin complexes (0 s, 125.3 s, 185.5 s and 227.5

s) in Supplementary Movie S6. Membrane fission occurred at flanking regions of a dynamin-amphiphysin cluster. Corresponding height profiles along the red line (shown in the 0 s image) passing through the two fission points (arrows marked with FP.1 and FP.2) are shown below, together with clustered dynamin-amphiphysin ring complexes (red arrowheads). (B) Height profiles at fission points (FP.1 and FP.2) over time before (Supplementary Movie S7) and after constriction (Supplementary Movie S6). The heights of the lipid tubules from the substrate surface were measured at the fission points. (C) Clips of HS-AFM images showing clustering dynamin-amphiphysin complexes and membrane constriction at flanking regions of the cluster (arrow). HS-AFM images are shown in pseudo color. Scale bar is 40 nm.

Figure 5. Amphiphysin contributes to generation of uniformly-sized vesicles by controlling dynamin-amphiphysin clusters (A) Representative EM images of membrane vesicles generated by dynamin-amphiphysin complexes (Dynamin + Amphiphysin) or dynamin alone (Dynamin) after addition of GTP. Size distribution of generated vesicles are shown in the right panel. The average sizes of vesicles were 69.98 ± 0.61 nm (mean diameter ± s.e.m., n>30, N=3) for dynamin-amphiphysin complexes and 204.57 ± 1.10 nm (mean diameter ± s.e.m., n>45, N=3) for dynamin alone. Scale bar is 200 nm. (B) Representative EM images of membrane constriction induced by dynamin-amphiphysin complexes (Dynamin + Amphiphysin) and dynamin alone (Dynamin) in the presence of GDP and vanadate. Distribution of intervals between constriction sites are quantified in the right panel. The average intervals of constriction sites induced are 150.28 ± 9.75 nm (mean intervals ± s.e.m., n=25 from 7 tubes) by dynamin-amphiphysin complexes and 193.5 ± 15.8 nm (mean intervals ± s.e.m., n=46 from 15 tubes) by dynamin alone. Scale bar is 200 nm. (C) Clustering of dynamin-amphiphysin complexes (Dynamin + Amphiphysin) and dynamin alone (Dynamin) on lipid nanotubes in the presence of GDP and vanadate. Clusters of Dynamin-amphiphysin rings are indicated (white brackets). Distribution of cluster size were shown as scattered plot in the right panel. Average size of the clusters formed by dynamin-amphiphysin complexes and dynamin alone are 34.22 ± 1.66 nm (mean cluster size ± s.e.m., n=36 from 7 tubes) and 59.27 ± 4.69 nm (mean cluster size ± s.e.m., n=30 from 5 tubes) respectively. Scale bar is 100 nm.

Figure 6. Clusterase model of membrane constriction and fission mediated by dynamin-amphiphysin complexes. (A) Assembly and alignment of dynamin-amphiphysin washer rings-like or helical polymers on membrane tubules in the presence of GTP. (B)

Dynamic longitudinal rearrangement of dynamin-amphiphysin rings to form clusters induced by GTP hydrolysis. (C) Constriction of the clustered dynamin-amphiphysin which may provide local tension and/or torsion and/or friction at the edge of the clusters to induce membrane constriction. (D) Membrane fission caused by disassembly of dynamin-amphiphysin complexes into oligomers upon release of GTP hydrolytic products.

Supplementary Movie S1. HS-AFM imaging of a LUV

Supplementary Movie S2. HS-AFM imaging of a lipid tubules induced from LUVs by dynamin-amphiphysin complexes

Supplementary Movie S3. HS-AFM imaging of cluster formation by dynamin-amphiphysin ring complexes

Supplementary Movie S4. Particle tracking of dynamin-amphiphysin ring complexes before GTP addition (frames from 5 s to 21 s in Supplementary Movie S3)

Supplementary Movie S5. Particle tracking of dynamin-amphiphysin ring complexes after GTP addition (frames from 38 s to 124 s in Supplementary Movie S3)

Supplementary Movie S6. HS-AFM imaging of constriction and fission of lipid tubules by dynamin-amphiphysin complexes

Supplementary Movie S7. HS-AFM imaging of lipid tubules before constriction and fission by dynamin-amphiphysin complexes

Supplementary Movie S8. HS-AFM imaging of constriction and fission of lipid tubules by dynamin-amphiphysin complexes

Figure 1.Takeda et al.

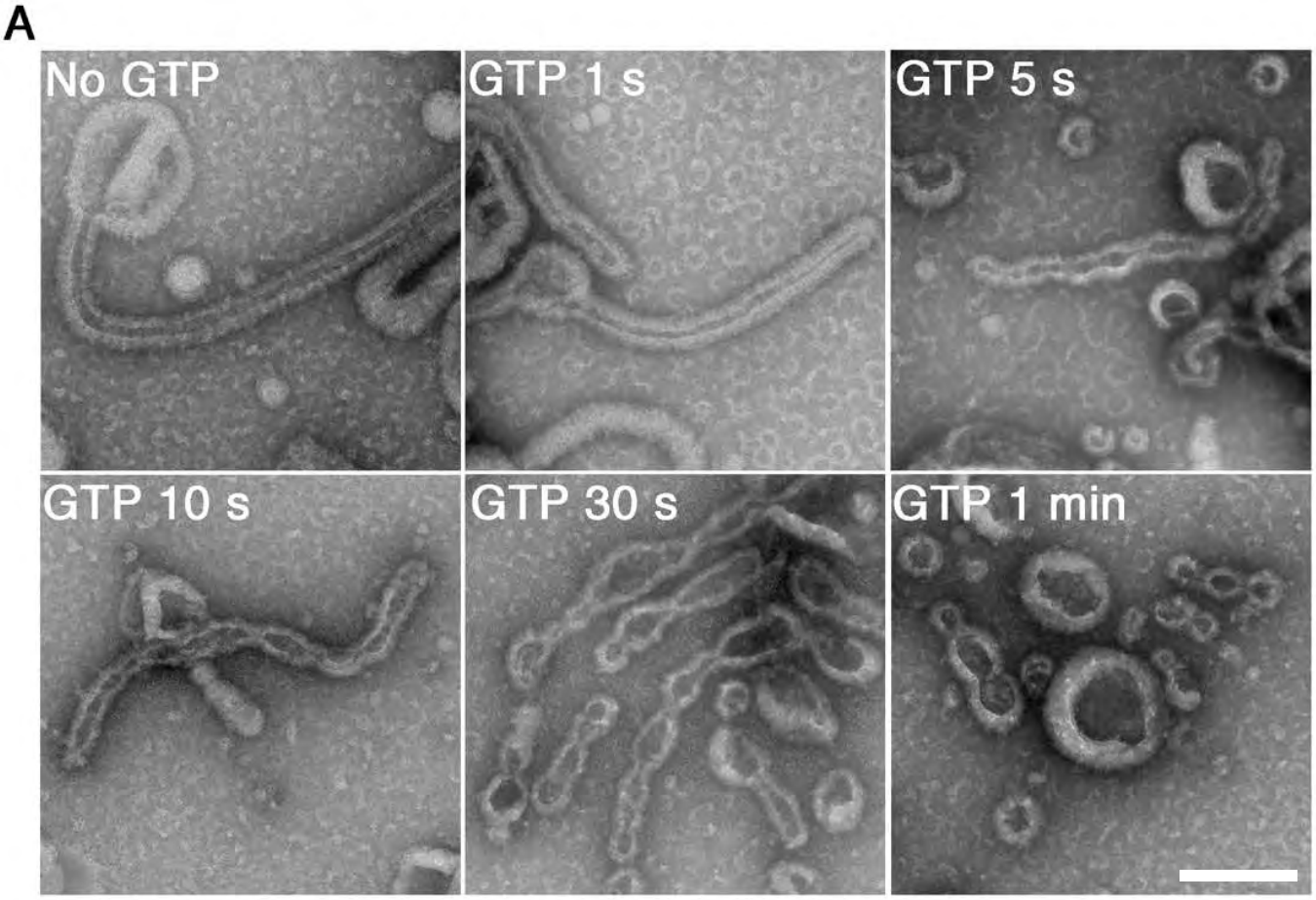

Figure 1-figure supplement 1.Takeda et al.

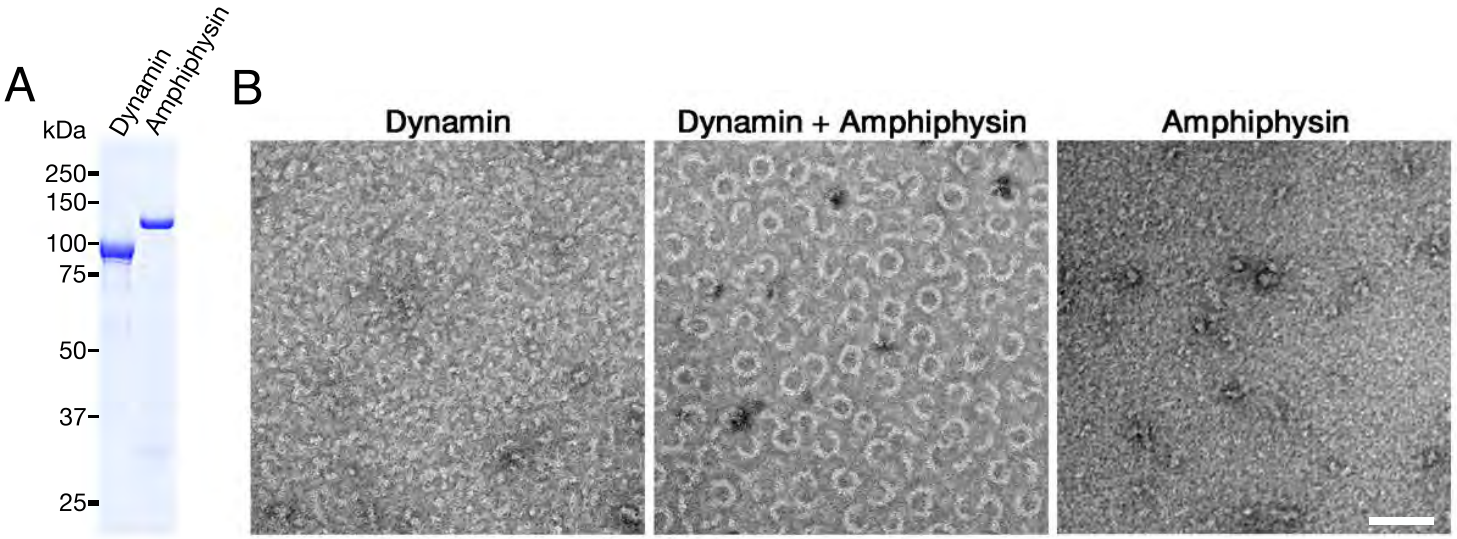

Figure 2.Takeda et al.

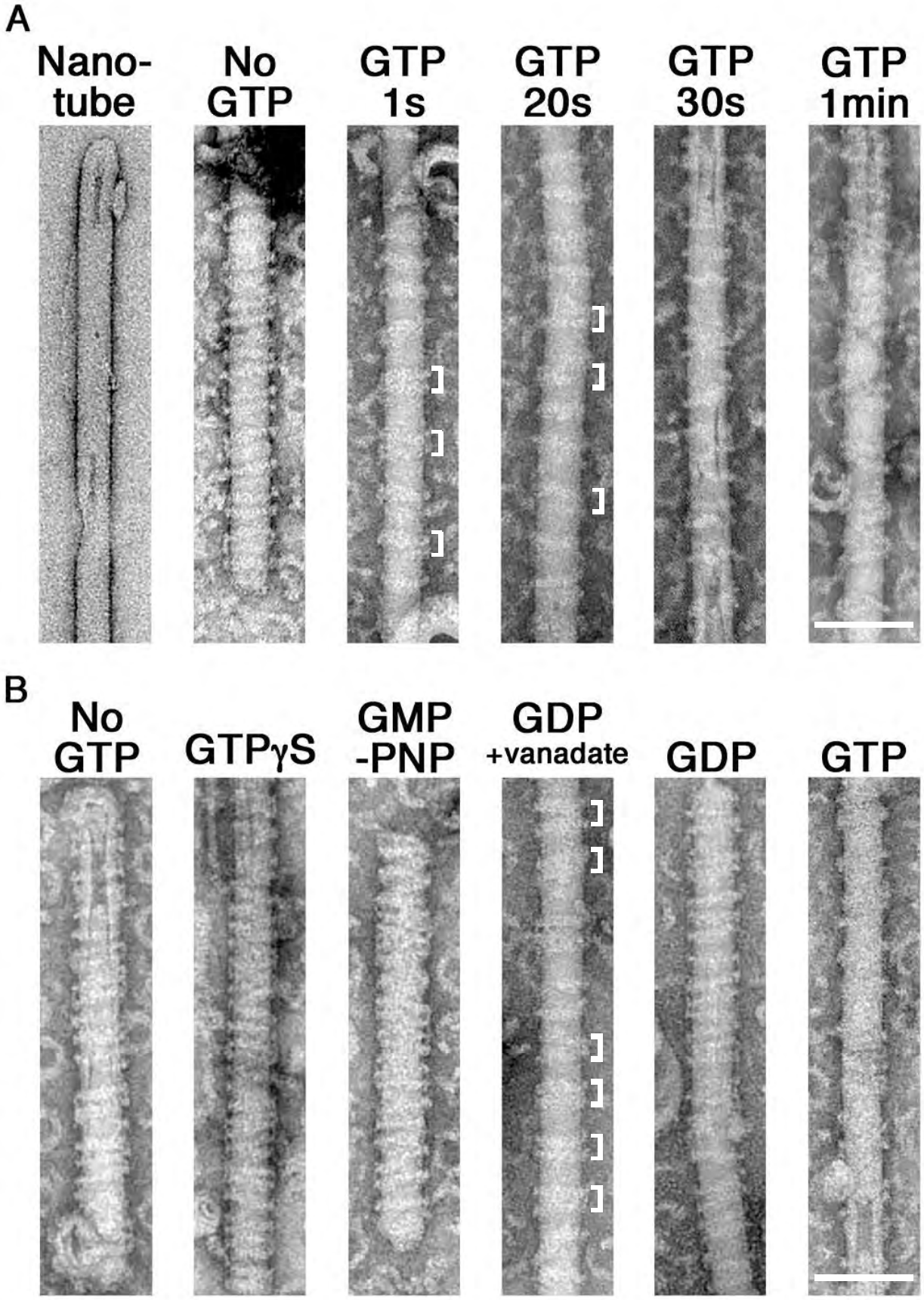

Figure 3.Takeda et al.

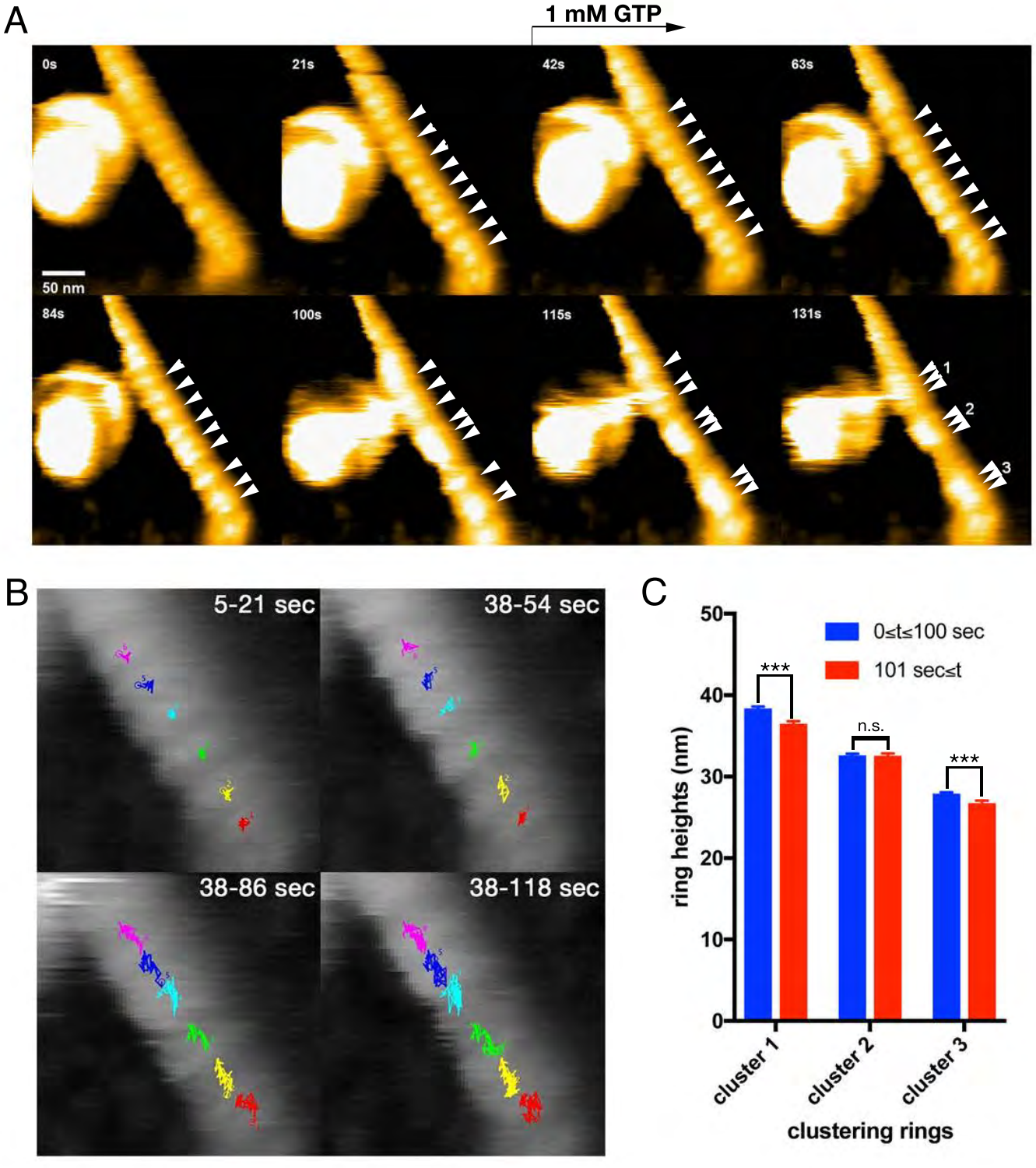

Figure 3-figure supplement 1.Takeda et al.

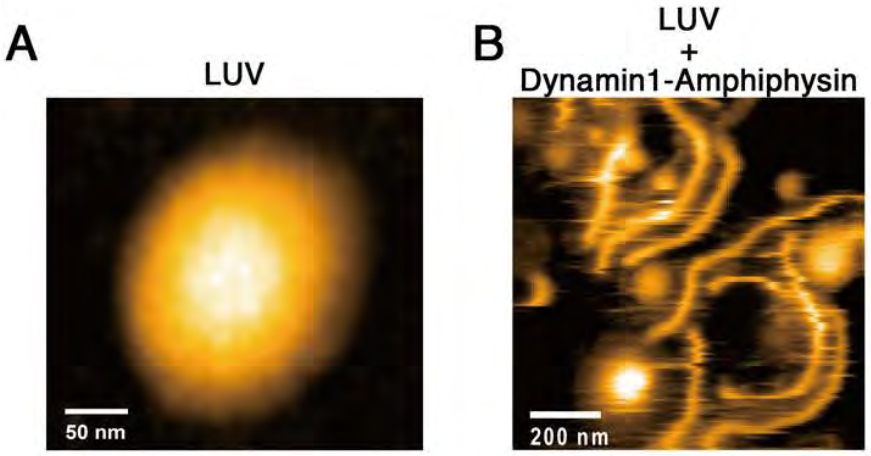

Figure 3-figure Supplement 2.Takeda et al.

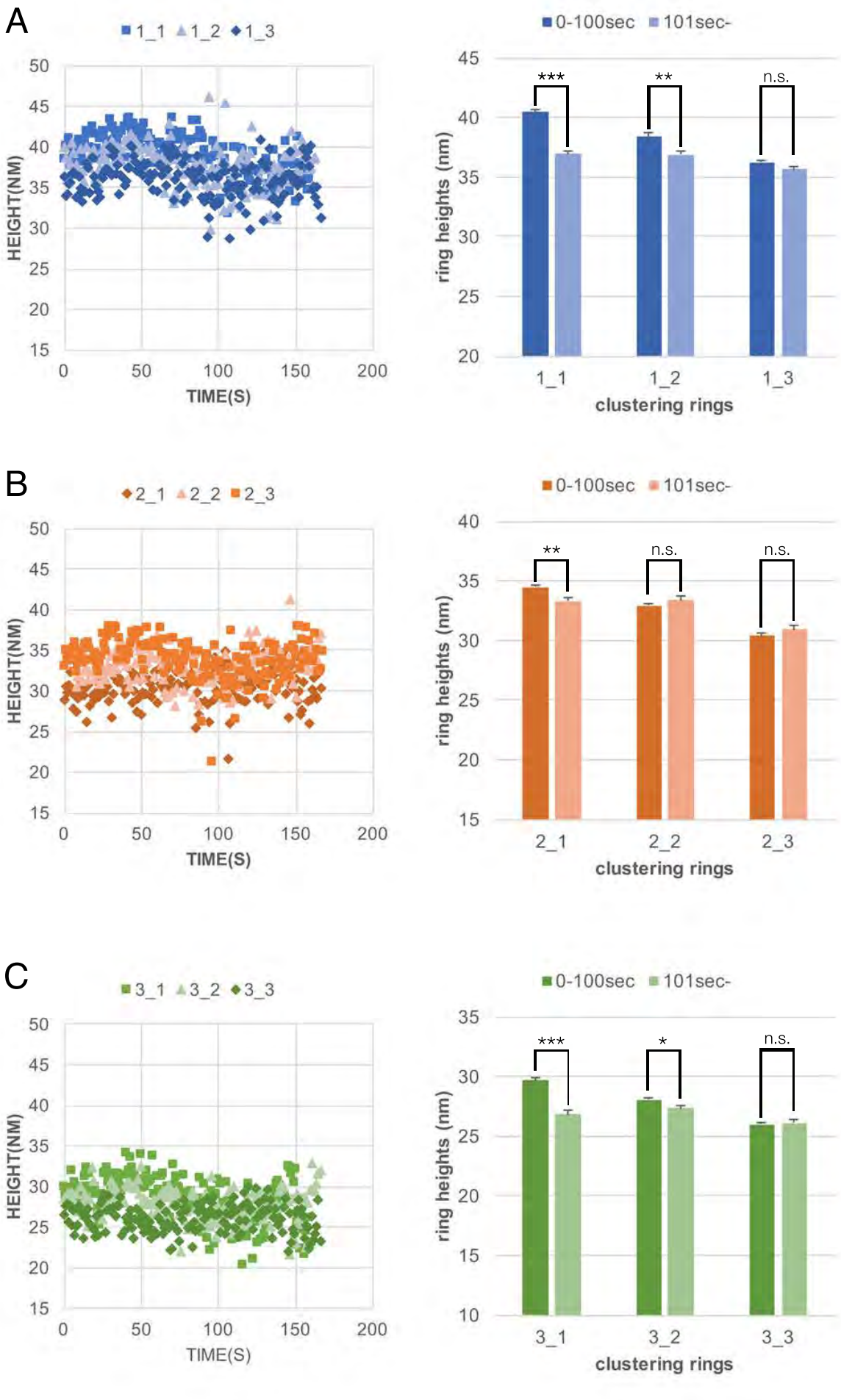

Figure 4.Takeda et al.

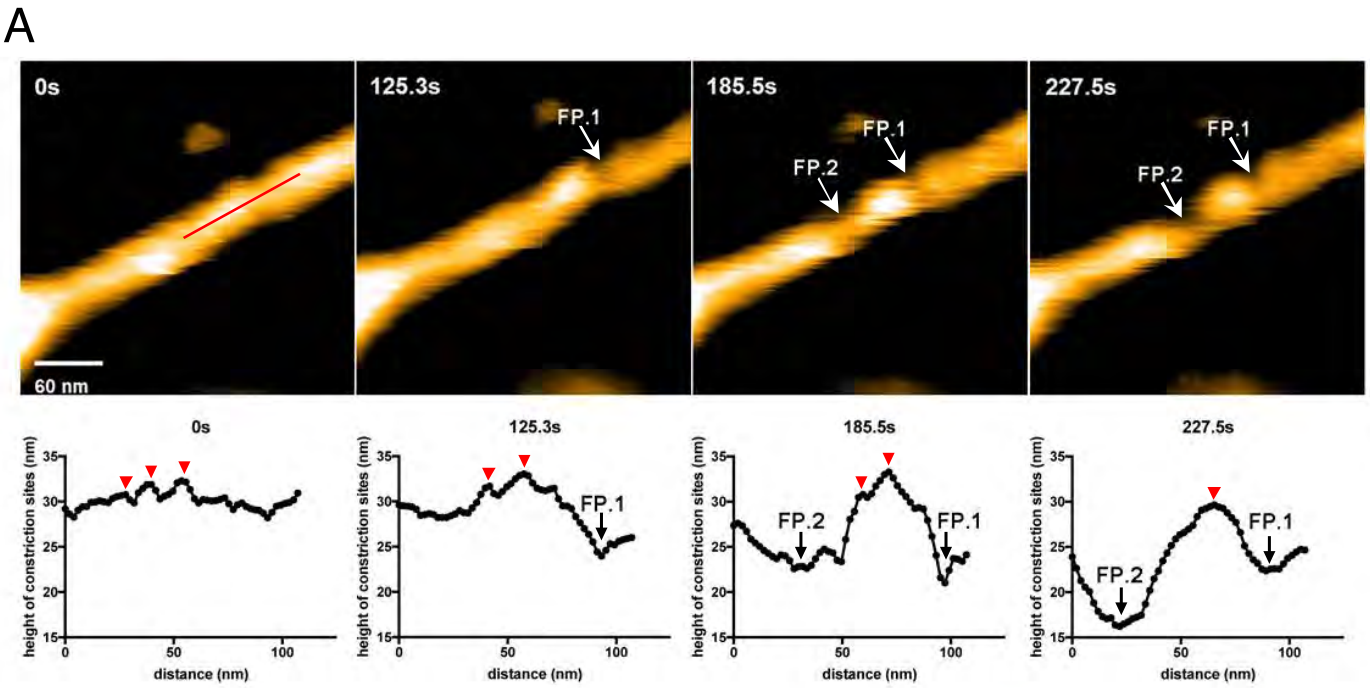

Figure 5.Takeda et al.